Clinical Science (2022) **136** 1691–1710
https://doi.org/10.1042/CS20220581

PORTLAND PRESS

Research Article

CEACAM5 inhibits the lymphatic metastasis of head and neck squamous cell carcinoma by regulating epithelial–mesenchymal transition via inhibiting MDM2

Xudong Wang[1,2], Yanshi Li[1], Min Pan[1], Tao Lu[1], Min Wang[1], Zhihai Wang[1], Chuan Liu[1] and Guohua Hu[1]

[1]Department of Otorhinolaryngology, the First Affiliated Hospital of Chongqing Medical University, Chongqing 400016, China; [2]Department of Otorhinolaryngology, The People's Hospital of Jianyang City, Jianyang, Sichuan 641400, China

Correspondence: Guohua Hu (2h4841@hospital.cqmu.edu.cn)

Lymph node (LN) metastasis affects both the management and prognosis of head and neck squamous cell carcinoma (HNSCC). Here, we explored the relationship between lymphatic metastasis and CEA family member 5 (CEACAM5), including its possible regulatory role in HNSCC. The levels of CEACAM5 in tissues from patients with HNSCC, with and without LN metastases, were assessed by transcriptome sequencing. The associations between CEACAM5 and the N stage of LN metastasis in HNSCC were predicted through The Cancer Genome Atlas (TCGA) and Gene Expression Omnibus (GEO) databases and a pan-cancer analysis of CEACAM5 expression in 33 common human tumors was conducted. CEACAM5 levels were analyzed in tumor and normal tissue specimens from HNSCC patients and the correlation between CEACAM5 levels and prognosis was evaluated. The influence of CEACAM5 on cell proliferation, invasion, migration, and apoptosis was investigated in HNSCC cell lines, as were the downstream regulatory mechanisms. A mouse model of LN metastasis was constructed. CEACAM5 levels were significantly higher in HNSCC tissue without LN metastasis than in that with LN metastasis. Similar findings were obtained for the clinical specimens. CEACAM5 levels were associated with better clinical prognosis. CEACAM5 was found to inhibit the proliferation and migration and promote the apoptosis of HNSCC cells. A mouse xenograft model showed that CEACAM5 inhibited LN metastasis. In conclusions, CEACAM5 inhibited epithelial–mesenchymal transition (EMT) in HNSCC by reducing murine double minute 2 (MDM2) expression and thereby suppressing LN metastasis. CEACAM5 has potential as both a prognostic marker and a therapeutic target in HNSCC.

Introduction

Head and neck squamous cell carcinoma (HNSCC) originates from mucosal epithelial cells in the mouth, pharynx, and larynx [1] and affects approximately 600000 people per year worldwide [2,3]. Oral cavity tumors and laryngeal cancer are often associated with excessive tobacco and alcohol consumption, while there is growing evidence that pharyngeal cancer is linked to human papillomavirus (HPV) infection, mainly HPV-16 [4]. Moreover, HPV-negative and HPV-positive HNSCC differ both genetically and in clinicopathological appearance [5]. More than 50% of patients with HNSCC have locally advanced lesions at first diagnosis and between 60 and 80% of them exhibit lymph node (LN) metastasis when starting treatment [6–9]. Despite the availability of a variety of comprehensive therapeutic options, the prognosis of HNSCC patients remains poor, with a five-year survival of approximately 60% for patients with laryngeal

Received: 31 August 2022
Revised: 14 November 2022
Accepted: 14 November 2022

Accepted Manuscript online: 15 November 2022
Version of Record published: 25 November 2022

Clinical Science (2022) **136** 1691–1710
https://doi.org/10.1042/CS20220581

cancer and 25% for those with hypopharyngeal cancer [10–12]. Accordingly, novel strategies are needed for the effective prevention and treatment of LN metastasis.

RNA sequencing is widely used in both cancer diagnosis and research into therapeutic strategies for this disease [13,14], including the exploration of biomarkers and the characterization of cancer heterogeneity, drug resistance, and the immune microenvironment [15–17]. Single-cell sequencing has shown that the epithelial–mesenchymal transition (EMT) signature can independently predict LN metastasis, cancer grade, and adverse pathological features [18,19]. The CEA family member 5 (CEACAM5) family of proteins includes both membrane junction and secretory glycoproteins. Membrane junction glycoproteins are either embedded within membranes via glycosylphosphatidylinositol (GPI) anchors or attached to the cell surface through transmembrane domains. GPI-anchored family members include CEACAM5, CEACAM6, CEACAM7, and CEACAM8 [20]. CEACAM5 is involved in the regulation of cell differentiation, apoptosis, and cell polarity, and can thus affect tumor development [21]. This protein can also serve as a biomarker of gastrointestinal cancer [22]. Murine double minute 2 (MDM2) is a RING-domain E3 ubiquitin ligase that, when phosphorylated, translocates to the nucleus, where it regulates the expression of a variety of genes in both tumor and normal cells [23]. Interaction between the NH2-terminal domain of MDM2 and the α-helix in the NH2-terminal domain of p53 induces the degradation of the latter, thereby promoting carcinogenesis [24].

EMT involves the acquisition of mesenchymal features by epithelial cells and is normally active during tissue development and repair, as well as stem cell functions [25]. EMT reactivation is associated with tumorigenesis, cancer cell invasion and metastasis, and drug resistance [26–28]. This transformation in function is largely regulated by the transcription factors Twist, Slug, Snail, and ZEB1. In addition, EMT can inhibit cell senescence and apoptosis and increase the tolerance to radiotherapy and chemotherapy [29,30].

In the present study, CEACAM5 expression was observed to be significantly lower in both HNSCC samples and cell lines. Importantly, we found that CEACAM5 inhibits HNSCC lymphatic metastasis by negatively regulating MDM2 expression and thereby inhibiting EMT both *in vivo* and *in vitro*. These findings provide insights into the function of CEACAM5 in HNSCC.

Methods

Tissues and patient data

Fresh HNSCC and adjacent normal tissue specimens were collected from patients undergoing tumor resection in the First Affiliated Hospital of Chongqing Medical University between 2014 and 2022. The specimens included 57 paraffin-embedded tumor tissues that were used for histological analysis. Patients who had received preoperative antitumor therapy such as radiotherapy or chemotherapy were excluded. The study was carried out in accordance with the Declaration of Helsinki and was authorized by the Ethics Committee of the First Affiliated Hospital of Chongqing Medical University.

RNA extraction and quantitative reverse transcription-PCR

Total RNA was extracted from fresh frozen samples using an E.Z.N.A. Total RNA Kit I (Omega Bio-Tek, U.S.A.). The extracted RNA was reverse transcribed into cDNA (37°C for 15 min, 70°C for 5 min) using a PrimeScript RT Reagent Kit (Takara, Dalian, China). Quantitative-PCR (qPCR) was performed with the SYBR PrimeScript RT-PCR Kit (Takara). GAPDH served as the internal control and relative gene expression levels were calculated using the $2^{-\Delta\Delta Ct}$ method. The sequences of the primers used for qPCR are shown in Additional file 1: Supplementary Table S1.

Protein extraction and western blotting

Total protein was isolated using a protein extraction kit (KGP250, KeyGen, Jiangsu, China). The lysates were centrifuged and the protein concentration in the supernatants was measured using the BCA method (P0010S, Beyotime, Shanghai, China). Equal amounts of protein were separated via 10% SDS-PAGE and electroblotted onto polyvinylidene fluoride (PVDF) membranes. After blocking, the membranes were incubated overnight at 4°C with primary antibodies targeting CEACAM5 (Abcam, U.S.A.), MDM2 (Cell Signaling Technology, U.S.A.), E-cadherin (Cell Signaling Technology), N-cadherin (Cell Signaling Technology), vimentin (Cell Signaling Technology), LYVE-1 (Abcam), and GAPDH (Abcam). After washing, the membranes were incubated with a secondary antibody for 1 h at room temperature. An enhanced chemiluminescence (ECL) kit (Thermo, Shanghai, China) was used for visualization. Detailed antibody information is provided in Additional file 2: Supplementary Table S2.

Immunohistochemistry

An immunohistochemistry (IHC) kit (SP-9000, Beijing, Zhongshan Jinqiao, China) was used to stain 4-μm-thick paraffin-embedded tumor sample sections. Specifically, after dewaxing and rehydration in fresh xylene and a graded alcohol series, antigen retrieval was performed with citrate buffer at 95°C for 15 min, followed by incubation with an endogenous peroxidase blocker for 15 min at 37°C. The sections were then incubated first with primary antibodies overnight at 4°C and then with HRP-conjugated streptavidin (100 μL) for 15 min, followed by counterstaining with hematoxylin and visualization with diaminobenzidine (DAB). Different fields of view of each section were randomly imaged under a light microscope at ×200 magnification. Gray levels were estimated in ImageJ and graded as follows: 0, negative; 1–3, weak; 4–5, medium; and 6–7, strong.

Cell culture

FaDu and SCC15 cells were obtained from the Cell Bank of the Chinese Academy of Sciences (Shanghai, China). Cells were grown in Dulbecco's Modified Eagle's Medium (DMEM; Gibco, MA, U.S.A.) containing 10% fetal bovine serum (FBS; Gibco, Australia) and 1% penicillin/streptomycin (Beyotime, Shanghai, China) at 37°C with 5% CO_2.

RNA interference and cell transfection

The siRNA used in the present study was obtained from GenePharma (Shanghai, China). Cells were seeded in 6-well plates (2.5×10^5 cells per well) and allowed to grow to between 60 and 70% confluence. The cells were then transfected with siRNA using Lipofectamine iMAX (Invitrogen, U.S.A.) and incubated in serum-free DMEM for 6 h. The medium was then replaced with DMEM supplemented with 10% FBS and the cells were cultured for a further 48–72 h. RNA and protein were extracted for the assessment of transfection efficiencies as well as to select the best sequence for use in subsequent experiments.

Lentiviral vectors and cell transduction

To knock down CEACAM5, short hairpin RNA (shRNA)-targeting human CEACAM5 was cloned into the hU6-MCS-Ubiquitin-firefly_Luciferase-IRES-puromycin lentiviral vector (GV344, Genechem, Shanghai, China). For CEACAM5 overexpression, full-length CEACAM5 cDNA was cloned into the Ubi-MCS-firefly_Luciferase-IRES-Puromycin lentiviral vector (GV260, Genechem). Specifically, cells were grown in 6-well plates (1×10^5 cells per well) to between 20 and 30% confluence. Lentivirus was transfected into the cells at a multiplicity of infection (MOI) of 10 using HiTransG A/P infection-enhancing solution. After 24 h, the cells were incubated in DMEM with 10% FBS and 2 μg/mL puromycin for 1 week, followed by selection.

Colony formation assay

Colony formation assays were used to assess the tumorigenic ability of the cells. Stably lentivirus-transduced FaDu and SCC15 cells were seeded in 6-well plates (1000 cells/well and 650 cells/well, respectively) in DMEM with 10% FBS and grown for approximately 2 weeks. The medium was replaced every 4 days. The cells were subsequently fixed in 4% paraformaldehyde and stained with 0.1% crystal violet for 20 min, and the number of colonies was counted.

Transwell migration and invasion assays

The migratory and invasive potential of the cells was assessed using 8-μm-pore Transwell inserts (Corning, U.S.A.) coated or not with Matrigel (BD Biosciences, San Jose, CA, U.S.A.). Specifically, 1×10^5 cells were suspended in 200 μL of serum-free medium and placed in the upper chamber of the inserts. The lower chamber contained 600 μL of DMEM supplemented with 15% FBS. After incubation for 24 h, cells remaining on the upper chamber of the membrane (unmigrated cells) were wiped off with a cotton swab. Cells that had crossed the membrane (migrated cells) were fixed in 4% paraformaldehyde and stained with 0.1% crystal violet for 20 min. The number of migrated cells was counted under a microscope.

Flow cytometry

For the analysis of apoptosis, an Annexin V-FITC/PI Detection Kit (SunGENE BioTEch, Tianjin, China) was used to label apoptotic cells. Cells were grown in 6-well plates (1×10^5/well) to 90% confluence, harvested, and subjected to flow cytometry (FCM; BD Biosciences, U.S.A.). For the cell cycle assay, stably transfected cells were fixed in 70% ice-cold ethanol overnight at 4°C, incubated with RNase A and propidium iodide, and then analyzed in a flow cytometer.

Clinical Science (2022) **136** 1691–1710
https://doi.org/10.1042/CS20220581

EdU proliferation assay

An EdU detection kit (RiBoBio, Guangzhou, China) was used for the cell proliferation assay. Briefly, cells were grown in 6-well plates to 70–80% confluence and then incubated with EdU (50 μM) at 37°C for 2 h. The cells were subsequently fixed in 4% paraformaldehyde, stained with Apollo for 30 min, and imaged under an inverted microscope.

Plasmid transfection and wound-healing assay

A total of 2.5×10^5 cells were seeded per well of a 6-well plate, allowed to grow to 60–70% confluence, and then transfected using a liposome transfection kit (NEOFECTTMDNA transfection reagent, Beijing, China). The medium was replaced after 24 h and the cells were grown to approximately 95% confluence. A 200-μL pipette tip was used to make four scratches in the cell monolayer. After being allowed to grow for 24 h in serum-free DMEM, the cells were imaged under an inverted microscope.

Generation of an animal model of inguinal LN metastasis

Experiments involving mice were performed at a specific pathogen-free facility at Chongqing Medical University. Male BALB/c nude mice aged between 4 and 6 weeks were purchased from HFK Bioscience Limited Company (Beijing, China). SCC15 cells (5×10^6 in 40 μL of PBS) transfected with the empty vector or the CEACAM5 overexpression plasmid were injected into the foot pads of the mice. After 35 days, the mice received intraperitoneal injections of 15 mg/mL D-Luciferin (Beyotime). Mice were monitored using *in vivo* bioluminescence imaging and, following euthanasia, the foot pad tumors and ipsilateral inguinal LNs were collected for further analysis.

Bioinformatics

Transcriptome sequencing was performed on 11 tumor tissues from HNSCC patients with or without LN metastasis [31]. Differentially expressed genes (DEGs) were identified using a threshold of $P<0.05$ and volcano plots were drawn using the Enhanced Volcano package in R. Protein–protein interaction (PPI) networks for genes related to CEACAM5 were compiled using the STRING database (https://cn.string-db.org/) [32] and visualized in Cytoscape [33]. GO enrichment analysis of the DEGs was performed through the Network Analyst database (https://www.networkanalyst.ca/) [34]. The HNSCC high-throughput sequencing datasets were downloaded from The Cancer Genome Atlas (TCGA) (https://portal.gdc.cancer.gov/) and Gene Expression Omnibus (GEO) databases (dataset GSE2379, platform GPL91).

Statistical analysis

GraphPad Prism version 8.0 (GraphPad Software, U.S.A.) and SPSS 20.0 (IBM Corp, NY, U.S.A.) were used for statistical analysis. *T*-tests were used for comparisons between two groups. One-way ANOVA was used for univariate comparisons among three or more groups. Multivariate between-group analysis was performed using two-way ANOVA. Pearson χ^2 tests were used to assess correlations between CEACAM5 expression and clinicopathological features. Kaplan–Meier and logarithmic rank analyses were used to evaluate prognostic factors. All data were expressed as means ± standard deviation (SD). A *P*-value <0.05 was considered significant.

Results

Low CEACAM5 expression in HNSCC is associated with LN (N) stage

To explore the role of CEACAM5 in human HNSCC, transcriptome sequencing was performed on six HNSCC tissues with LN metastases and five without. A total of 2294 DEGs between the two tissue types were identified (shown in the heatmap in Figure 1A and the volcano plot in Figure 1C). Expression profile microarray data for ten HNSCC cases with and four without LN metastases were obtained from the GEO database (depicted in the heatmap in Figure 1B). Analysis of the data indicated that CEACAM5 expression was lower in cases with LN metastases than in those without. We then conducted a pan-cancer analysis of CEACAM5 levels in 33 common human cancers together with an assessment of the disease risk ratio. We found that the levels of CEACAM5 were significantly higher in normal tissues ($n=44$) than in HNSCC tissues ($n=520$) and that the CEACAM5 risk ratio in HNSCC was less than 1 ($P<0.05$) (Figure 1D,E). In addition, CEACAM5 expression in HPV-positive HNSCC was higher than that in HPV-negative HNSCC (Figure 1D). These findings indicated that CEACAM5 may act as a tumor suppressor in HNSCC. The mRNA levels of CEACAM5 were markedly higher in normal tissues than in tumor tissues and were also higher at the N0 stage than at the N1 and N3 stages based on TCGA data (Figure 1F). Survival analysis based on the same dataset confirmed that high CEACAM5 levels were associated with better overall survival (OS), disease-free survival, and

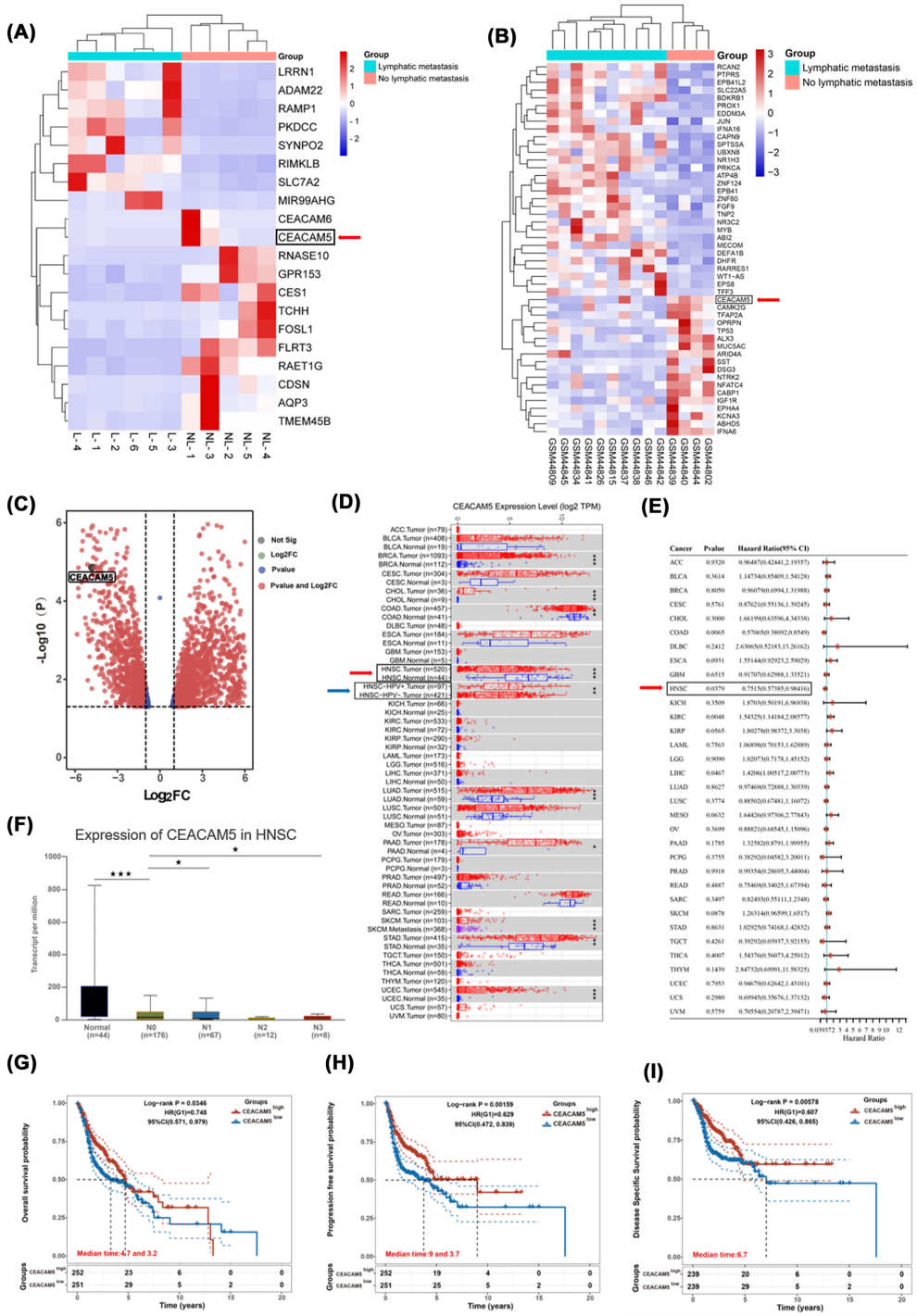

Figure 1. Low CEACAM5 expression in HNSCC is associated with lymph node (N) stage

(**A,C**) Transcriptome sequencing was performed on HNSCC tissues and the results were visualized in a heatmap and volcano plot. CEACAM5 was identified as a DEG in HNSCC. L: HNSCC tissue with LN metastasis. NL: HNSCC tissue without LN metastasis. (**B**) Gene expression microarray data were downloaded from the GEO database and CEACAM5 was displayed in a heat map. The columns represent sample numbers and the rows represent genes. (**D**) CEACAM5 expression in 33 common human tumors and HPV correlation in HNSCC was analyzed based on data from TCGA database. (**E**) The risk ratio of CEACAM5 in 33 common human tumors was analyzed via a forest plot. (**F**) The CEACAM5 transcript levels were measured in 263 HNSCC and 44 normal tissues based on data from TCGA. N_X represents lymph node (N) stage. (**G–I**) Survival analysis relating to CEACAM5 in HNSCC based on data from TCGA. Abbreviations: OS, overall survival; PFS, progression-free survival; DSS, disease-specific survival. $^{*}P<0.05$, $^{**}P<0.01$, $^{***}P<0.001$.

Clinical Science (2022) **136** 1691–1710
https://doi.org/10.1042/CS20220581

Table 1 Correlation between CEACAM5 expression and clinicopathological characteristics of HNSCC patients

Characteristics	No. of cases (%)	CEACAM5 expression		X^2	*P*-value
		Low (*N*=33)	High (*N*=24)		
Age (y)					
<60	23 (40.4)	13	10	0.030	0.863
≥60	34 (59.6)	20	14		
Gender					
Male	56 (98.2)	33	23	1.400	0.237
Female	1 (1.8)	0	1		
Cigarette					
No	9 (15.8)	4	5	0.793	0.373
Yes	48 (84.2)	29	19		
Alcohol					
No	17 (29.8)	9	8	0.244	0.621
Yes	40 (70.2)	24	16		
T classification					
T1	3 (5.3)	2	1	3.186	0.364
T2	9 (15.8)	3	6		
T3	26 (45.6)	15	11		
T4	19 (33.3)	13	6		
N classification					
N0	17 (29.8)	6	11	12.494	0.006**
N1	8 (14.0)	2	6		
N2	27 (47.4)	21	6		
N3	5 (8.8)	4	1		
Pathologic differentiation					
Poor	14 (24.6)	10	4	1.508	0.470
Moderate	29 (50.9)	15	14		
Well	14 (24.6)	8	6		
LN metastasis					
No	17 (29.8)	6	11	5.076	0.024*
Yes	40 (70.2)	27	13		
Extranodal extension					
No	46 (80.7)	23	23	6.095	0.014*
Yes	11 (19.3)	10	1		

*$P<0.05$, **$P<0.01$

disease-specific survival (DSS) (Figure 1G–I). Combined, these findings suggested that CEACAM5 expression is significantly correlated with the N (LN) stage in HNSCC.

CEACAM5 expression is down-regulated in HNSCC tissue samples and is correlated with clinical prognosis

The sequencing datasets for 53 normal and 520 HNSCC tissues were downloaded from TCGA. Analysis of the data showed that CEACAM5 levels were significantly higher in normal tissue than in HNSCC tissue (Figure 2A). Next, we analyzed CEACAM5 mRNA levels in nine HNSCC specimens without and nine with LN metastases, as well as in control tissues. The results showed that CEACAM5 levels in the nonmetastasis group were higher than those in the metastasis group (Figure 2C). The CEACAM5 protein levels were consistent with the results of the mRNA analysis as determined by western blotting (WB) (Figure 2B,D) and further confirmed by IHC (Figure 2E–G). Subsequent univariate and multivariate Cox regression analyses indicated that CEACAM5 expression was a prognostic factor for HNSCC. The clinicopathological data are shown in Tables 1 and 2. Finally, survival analysis demonstrated that high CEACAM5 levels were linked with improved OS in patients with HNSCC (Figure 2H). Together, these findings indicated that CEACAM5 expression is down-regulated in HNSCC and that elevated CEACAM5 levels are associated with better clinical outcome.

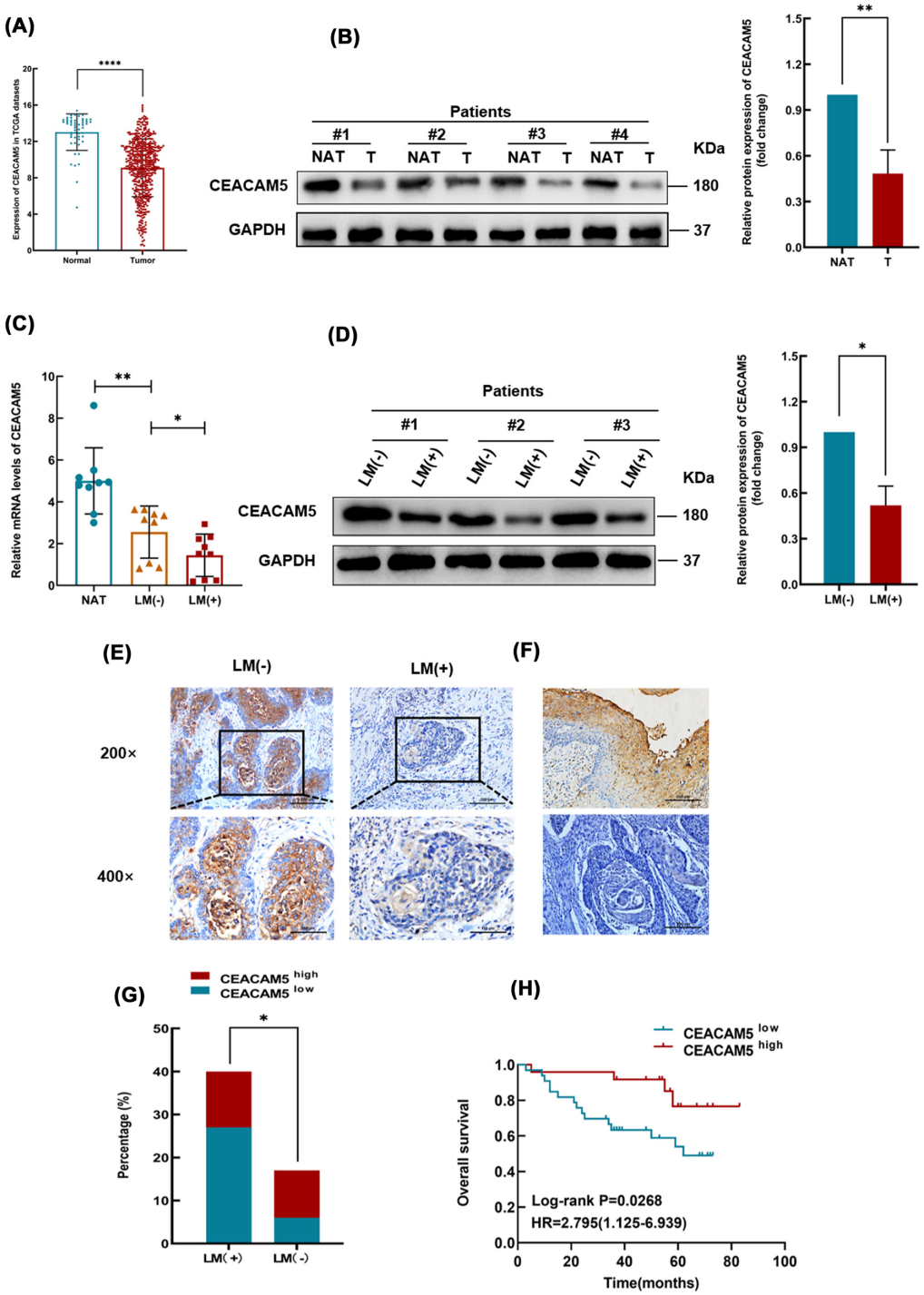

Figure 2. CEACAM5 expression is down-regulated in HNSCC tissue samples and is correlated with prognosis

(**A**) CEACAM5 expression was analyzed based on data from TCGA. (**B**) The protein expression of CEACAM5 in HNSCC tissues and adjacent normal tissues was analyzed by WB. NAT represents normal adjacent tissue, and T represents tumor tissue. (**C**) CEACAM5 expression in 18 HNSCC tissues with or without LN metastasis and adjacent normal tissues was analyzed by quantitative reverse transcription-PCR (qRT-PCR). LM(+) represents lymphatic metastasis, and LM(−) represents nonlymphatic metastasis. (**D**) CEACAM5 protein expression in HNSCC tissues with or without LN metastasis was assessed by WB. (**E**) The expression of CEACAM5 in 57 paraffin-embedded HNSCC tissue sections with or without lymphatic metastasis was analyzed via IHC. Scale bars: 200×, 200 μm; 400×, 100 μm. (**F**) Positive and negative controls. (**G,H**) Proportion distribution and survival curve relating to CEACAM5 expression in 57 HNSCC paraffin-embedded sections are shown. *P<0.05, **P<0.01, ***P<0.001, ****P<0.0001.

Clinical Science (2022) **136** 1691–1710
https://doi.org/10.1042/CS20220581

Table 2 Univariate and multivariate analyses of various prognostic parameters in patients with HNSCC Cox-regression analysis

Variables	Univariate analysis			Multivariate analysis		
	P	Hazard ratio	95% confidence interval	*P*	Hazard ratio	95% confidence interval
CEACAM5	0.036*	0.306	0.101–0.928	0.142	0.421	0.133–1.334
Age	0.440	0.701	0.284–1.727			
Gender	0.654	0.048	0.286–5.275			
Cigarette	0.660	1.391	0.320–6.044			
Alcohol	0.752	0.856	0.325–2.253			
T classification	0.005**	3.052	1.407–6.620	0.012*	2.807	1.250–6.303
N classification	0.026*	1.825	1.073–3.102	0.234	1.443	0.788–2.643
Pathologic differentiation	0.122	0.597	0.310–1.149			
LN metastasis	0.173	2.356	0.686–8.090			
Extranodal extension	0.013*	3.203	1.285–7.989	0.832	1.124	0.381–3.317

*$P<0.05$, **$P<0.01$

CEACAM5 inhibits the proliferation, migration, and invasion and promotes the apoptosis of HNSCC cells *in vitro*

Cell culture experiments were employed to assess the role of CEACAM5 in HNSCC. First, FaDu cells were transfected with three siRNAs targeting different sites in CEACAM5 (si-CEACAM5#1, si-CEACAM5#2, and si-CEACAM5#3), and the silencing efficiency of the siRNAs was assessed by qRT-PCR and WB (Figure 3A,B). Si-CEACAM5#1 displayed the best knockdown efficiency and was used for subsequent studies. Next, we established stable CEACAM5 overexpression and knockdown FaDu and SCC15 cell lines using lentiviral infection. Overexpression and knockdown efficiencies were confirmed at both the mRNA and protein levels (Figure 3C–F). EdU cell proliferation assays were performed on stably transfected HNSCC cells in the logarithmic growth phase. The results showed that the proliferative ability of CEACAM5-silenced cells (both the FaDu and SCC15 lines) was higher than that of the respective controls, whereas the opposite was observed in CEACAM5-overexpressing cells (Figure 3H,I). In addition, CEACAM5-silenced cells formed more and larger colonies compared with control cells (Figure 4A). CEACAM5-silenced cells also displayed increased migratory and invasive capacity relative to that of control cells; however, this trend was reversed in CEACAM5-overexpressing cells (Figure 4B,C). Additionally, compared with the respective controls, CEACAM5 overexpression increased the cell apoptosis rate, whereas CEACAM5 depletion exerted the opposite effect (Figure 4D). These data indicated that CEACAM5 inhibits the proliferation, survival, and motility of HNSCC cells.

The overexpression of CEACAM5 inhibits lymphatic metastasis *in vivo*

To evaluate the role of CEACAM5 in lymphatic metastasis *in vivo*, we xenografted SCC15 cells transfected with the empty vector or the CEACAM5 overexpressing plasmid into the foot pads of nude mice. The sizes and weights of the primary tumors and inguinal metastatic LNs were smaller in the CEACAM5-overexpressing group relative to those of the empty vector group (Figure 5A–E,G–I). Additionally, CEACAM5 overexpression reduced the LN metastatic potential of SCC15 cells (Figure 5F). CEACAM5 overexpression in the tumors was confirmed by qRT-PCR and WB (Figure 5J,K). Lastly, immunohistochemical analysis of the foot pad tumors showed greater staining intensities and proportion of CEACAM5 in tumors formed of CEACAM5-overexpressing cells, in contrast with reduced staining of LYVE-1 (Figure 5L). These findings indicated that CEACAM5 inhibits lymphatic metastasis *in vivo*.

CEACAM5 inhibits EMT in HNSCC cells

Numerous transcription factors have been implicated in tumorigenic processes. Among them, the EMT process is believed to be involved in tumor invasion and early metastasis. Accordingly, we used Spearman's correlations to assess the relationships between CEACAM5 and key EMT-related transcription factors in HNSCC based on high-throughput data from TCGA. The results showed that CEACAM5 was negatively associated with these transcription factors, especially Snail, Slug, and Twist (Figure 6A). In addition, qRT-PCR analysis of the stably transduced FaDu and SCC15 cells showed that, compared with the controls, the levels of the epithelial marker E-cadherin

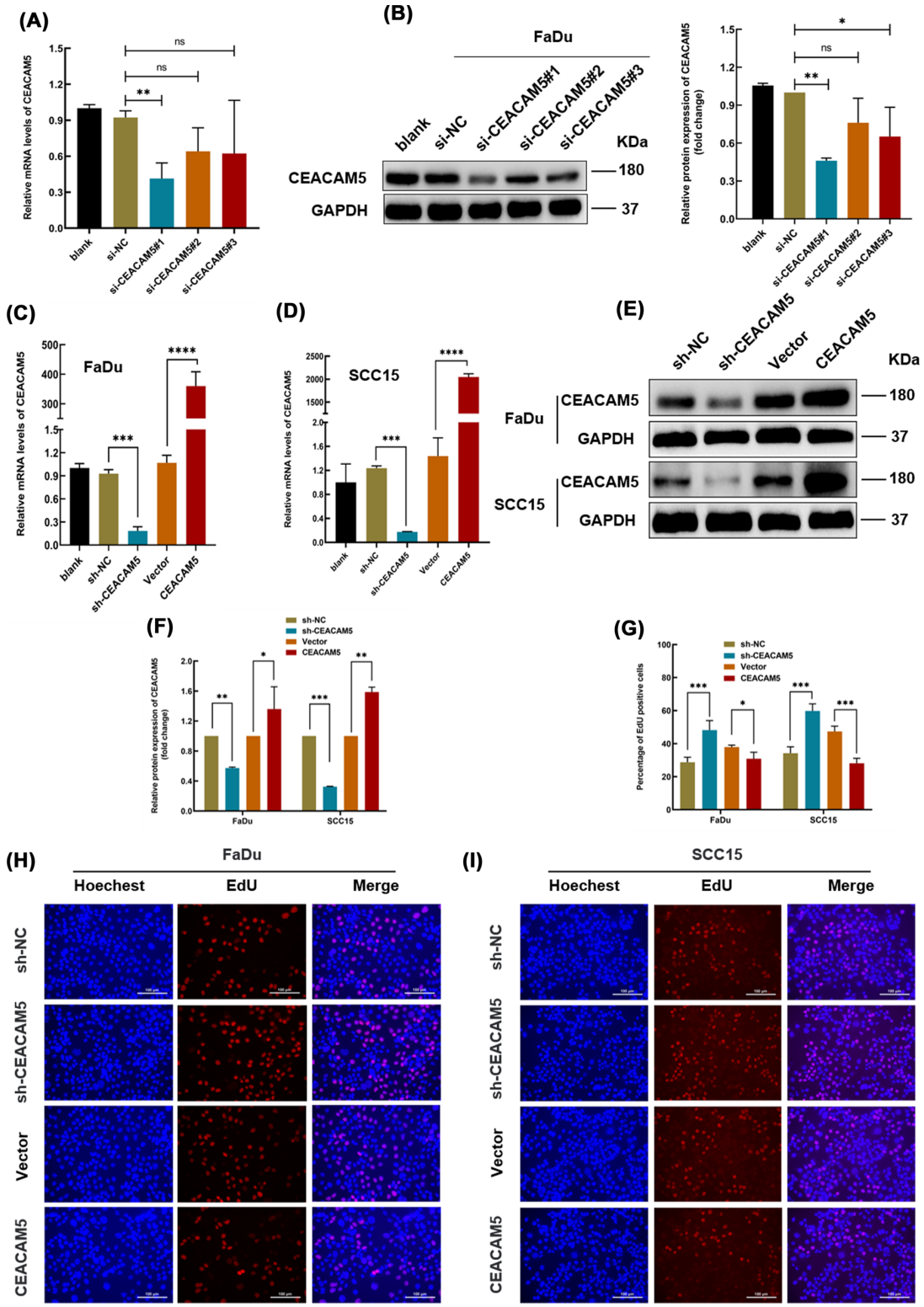

Figure 3. CEACAM5 inhibits the proliferative ability of HNSCC cells

(**A,B**) The efficiencies of the different siRNAs in silencing CEACAM5 expression in FaDu cells were screened by qRT-PCR and WB. CEACAM5 knockdown and overexpression efficiencies in stably transduced FaDu and SCC15 cells were detected by qRT-PCR (**C,D**) and WB (**E,F**). (**G–I**) Changes in the proliferative capacity of HNSCC cells after stable lentivirus-mediated transduction were investigated using an EdU proliferation assay. Scale bar: 100 μm. *$P<0.05$, **$P<0.01$, ***$P<0.001$, ****$P<0.0001$; Abbreviation: NS, not significant.

Clinical Science (2022) **136** 1691–1710
https://doi.org/10.1042/CS20220581

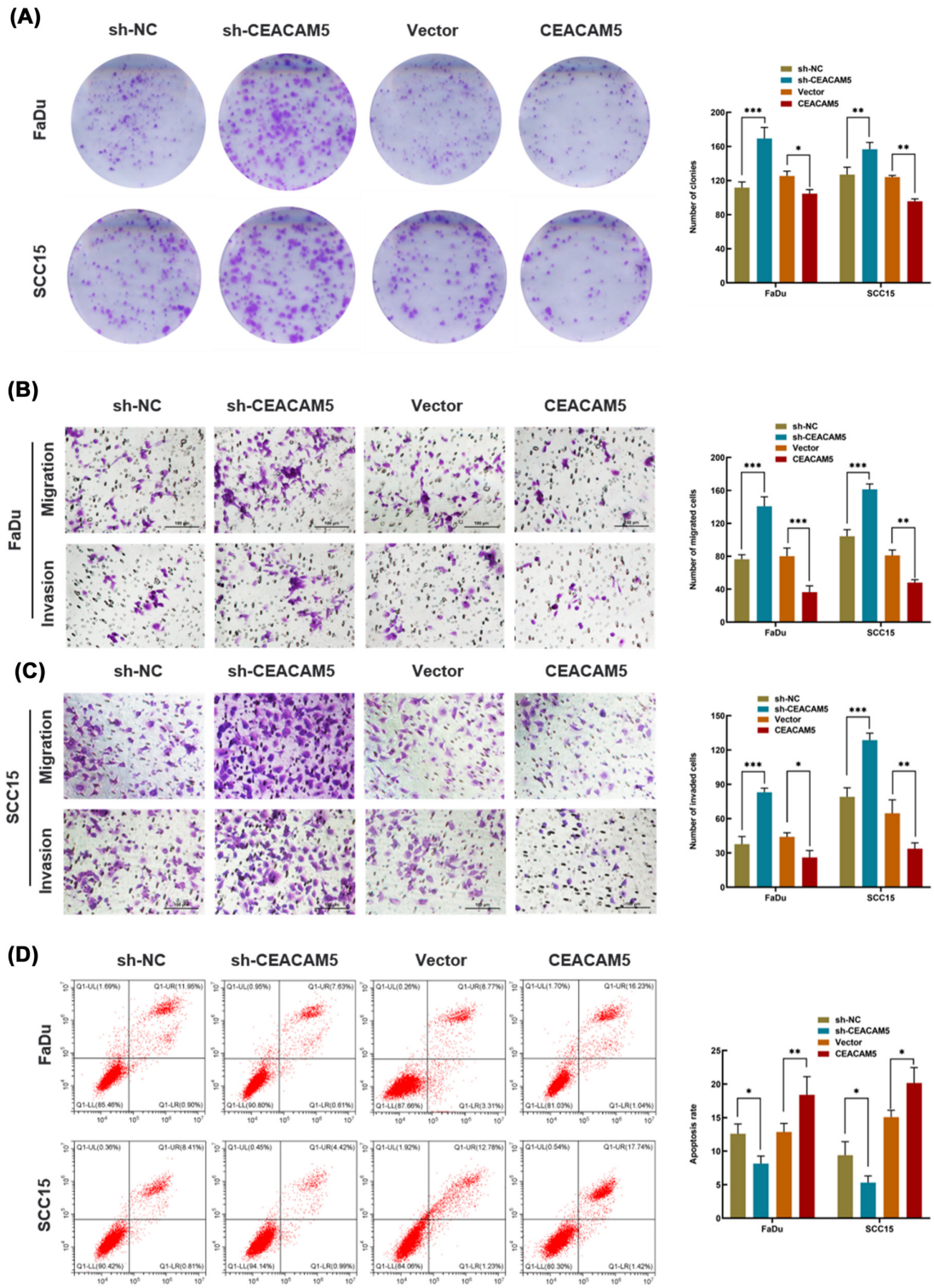

Figure 4. CEACAM5 inhibits proliferation, migration, and invasion and promotes apoptosis in HNSCC cells *in vitro*

(**A**) A colony formation assay was used to assess the tumorigenicity of HNSCC cells. (**B**) The migratory and invasive abilities of FaDu and SCC15 cells were assessed by Transwell assay. (**C**) Flow cytometry was used to measure the rate of apoptosis. The relevant statistics are displayed in the right panel. Scale bar: 100 μm. *$P<0.05$, **$P<0.01$, ***$P<0.001$.

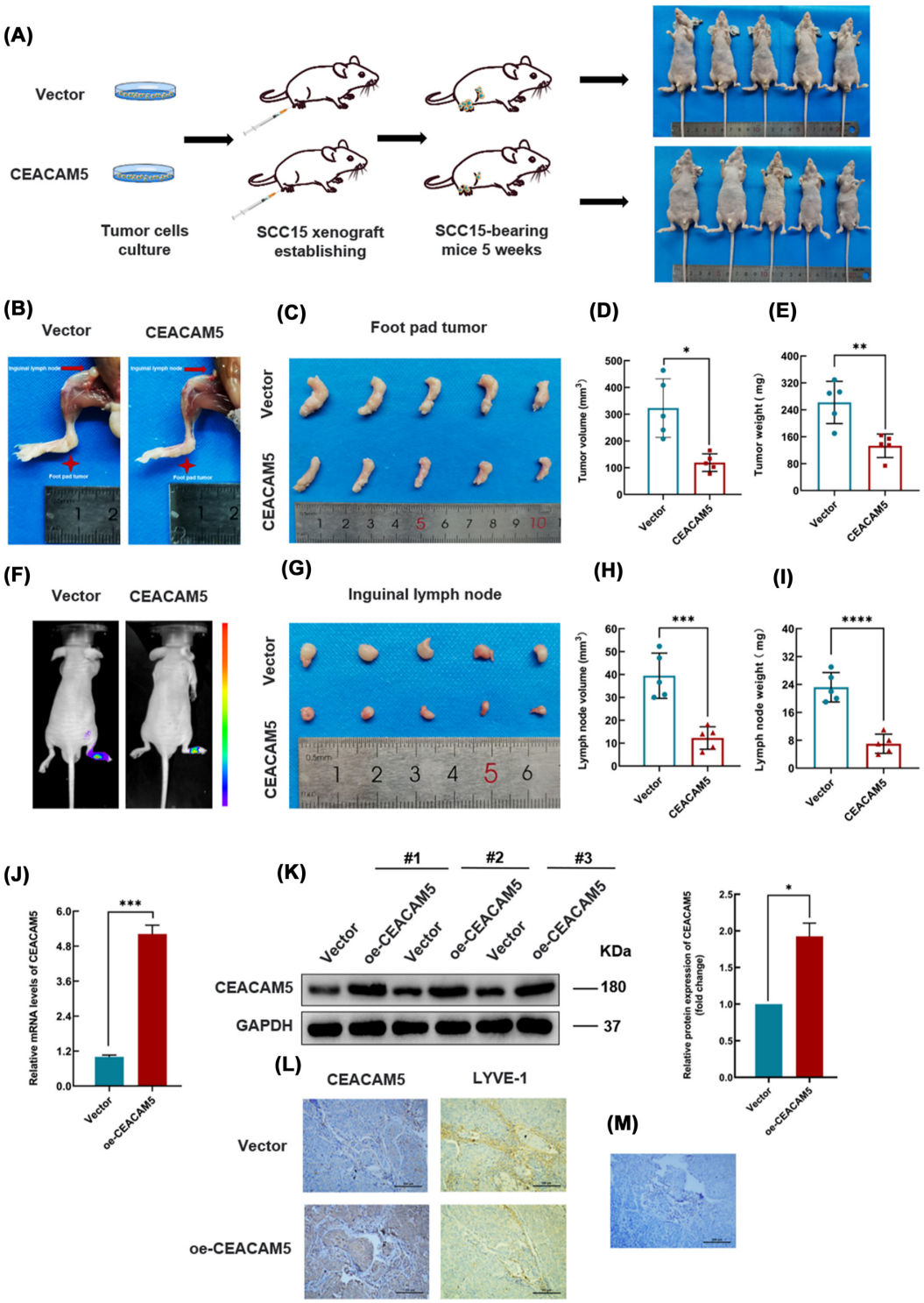

Figure 5. CEACAM5 overexpression inhibits lymphatic metastasis *in vivo*

(**A**) Procedure and animal grouping in the *in vivo* experiment. (**B**) Representative images of inguinal LN metastasis in nude mice. (**C,G**) Foot pad tumors and inguinal LNs collected from nude mice. (**D,E**) Foot pad tumor volumes and weights, respectively. (**H,I**) LN volumes and weights, respectively. (**F**) Representative bioluminescence images of inguinal LN metastasis in nude mice overexpressing CEACAM5. (**J,K**) The expression of CEACAM5 in foot pad tumors was analyzed by qRT-PCR and western blot. (**L**) The expression of CEACAM5 and the lymphangiogenesis factor LYVE-1 in primary tumor tissues of nude mice were evaluated by IHC. (**M**) Images of the negative control. Scale bar: CEACAM5, 200 μm; LYVE-1, 100 μm. *$P<0.05$, **$P<0.01$, ***$P<0.001$, ****$P<0.0001$.

Clinical Science (2022) **136** 1691–1710
https://doi.org/10.1042/CS20220581

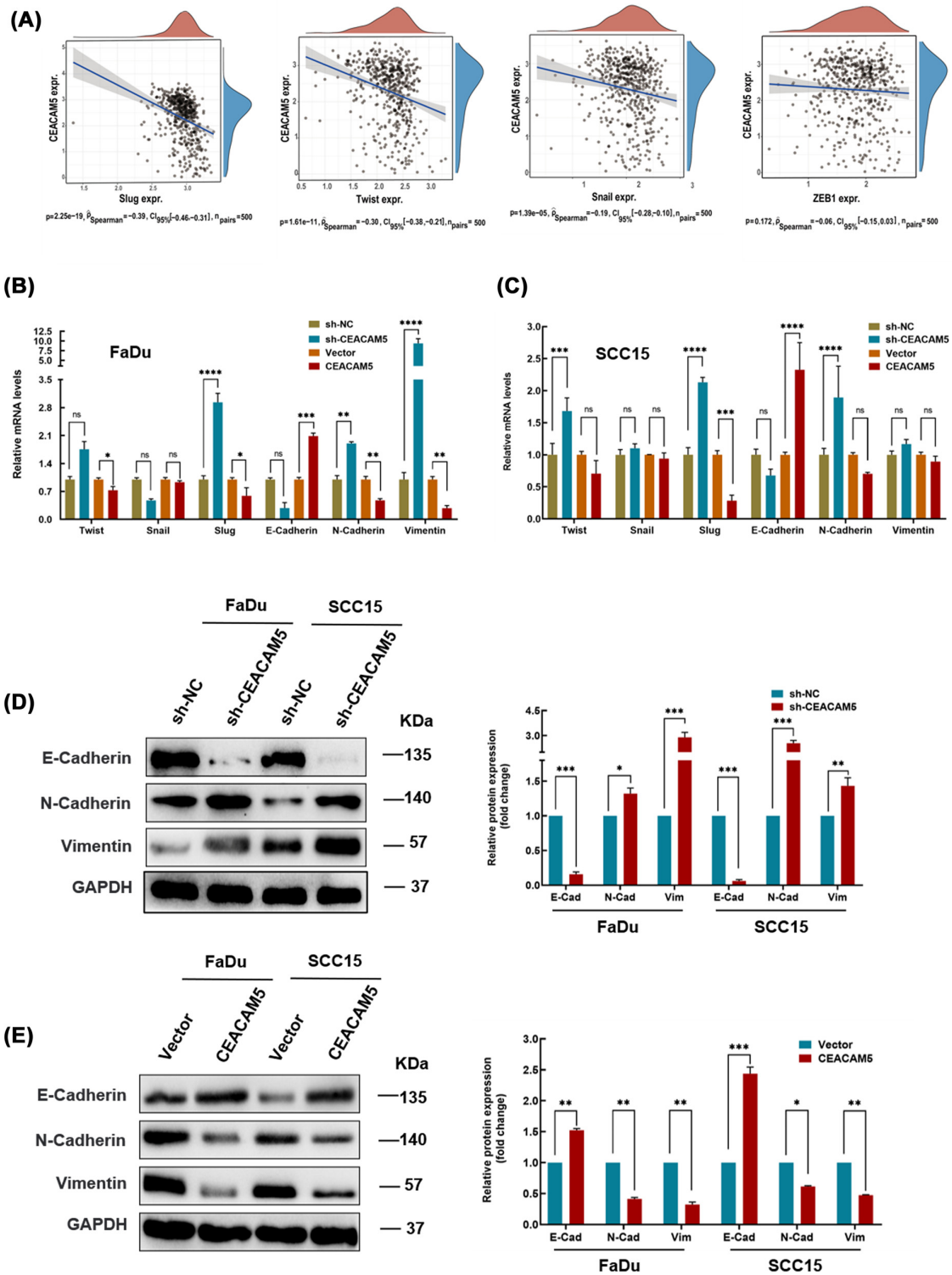

Figure 6. CEACAM5 inhibits EMT in HNSCC cells

(**A**) Spearman's correlation between the expression of EMT-related transcription factors and that of CEACAM5 was analyzed based on data from TCGA. (**B,C**) The mRNA expression levels of EMT-associated transcription factors and markers in stably transfected HNSCC cells were measured by qRT-PCR. (**D,E**) The protein expression levels of epithelial and mesenchymal markers in HNSCC cells after CEACAM5 knockdown or overexpression were detected by western blot. *$P<0.05$, **$P<0.01$, ***$P<0.001$, ****$P<0.0001$; Abbreviation: NS, not significant.

were reduced in CEACAM5-silenced cells, whereas those of key EMT-related transcription factors and the interstitial markers N-cadherin and vimentin were increased. In contrast, in CEACAM5-overexpressing cells, the mRNA levels of E-cadherin were up-regulated, while those of Slug, N-cadherin, and vimentin were suppressed, compared with that seen in cells transfected with the empty vector (Figure 6B,C). These findings were confirmed at the protein level (Figure 6D,E). These observations implied that CEACAM5 inhibits EMT in HNSCC cells.

CEACAM5 inhibits the expression of MDM2

It has been reported that the phosphorylation of MDM2 allows its entry into the nucleus where it regulates the expression of numerous genes [35,36]. Here, using the STRING database, we constructed a PPI network based on the HNSCC transcriptome-sequencing data (Figure 7H). CEACAM5 and MDM2 were seen to share many similarities in GO term enrichment in the Biological Process category (Figure 7A,B). In addition, we analyzed the expression of CEACAM5 and MDM2 in HNSCC based on data from TCGA and found that CEACAM5 levels were significantly higher in normal tissues than in tumor tissues, whereas the MDM2 levels showed the opposite trend (Figure 7C,E). This suggested that a negative regulatory relationship may exist between CEACAM5 and MDM2 (Figure 7D). To confirm this possibility, we next assayed the stably transfected FaDu and SCC15 cell lines for MDM2 expression using qRT-PCR, with the results showing that MDM2 expression was higher in CEACAM5-knockdown cells than in control cells. In contrast, MDM2 levels were lower in CEACAM5-overexpressing cells than in cells transfected with the empty vector (Figure 7F,G). These findings were confirmed by WB (Figure 7J). Furthermore, the MDM2 mRNA levels were lower in CEACAM5-overexpressing mouse xenograft tumors compared with the empty vector group (Figure 7I). These findings confirmed the existence of a negative regulatory relationship between CEACAM5 and MDM2.

MDM2 knockdown reverses the effect of CEACAM5 silencing on EMT

To further verify that a regulatory relationship indeed exists between CEACAM5 and MDM2, we silenced MDM2 in CEACAM5-knockdown cells. After puromycin selection for 1 week, the sh-CEACAM5-NC + sh-MDM2-NC, sh-CEACAM5-NC + sh-MDM2, sh-CEACAM5 + sh-MDM2-NC, and sh-CEACAM5 + sh-MDM2 SCC15 cell lines were constructed. We found that the mRNA level of the epithelial marker E-cadherin in sh-CEACAM5-NC + sh-MDM2 cells was increased in comparison with that in sh-CEACAM5-NC + sh-MDM2-NC cells. Moreover, the E-cadherin level was reduced in sh-CEACAM5 + sh-MDM2-NC cells compared with that in sh-CEACAM5-NC + sh-MDM2 cells and was higher in sh-CEACAM5 + sh-MDM2 cells than in sh-CEACAM5 + sh-MDM2-NC cells. Meanwhile, the mRNA expression levels of the EMT-related transcription factors as well as those of the interstitial proteins N-cadherin and vimentin displayed the opposite trend to that of E-cadherin (Figure 8A). These results were confirmed at the protein level (Figure 8B). Thus, the EMT process in cells in which both CEACAM5 and MDM2 were silenced was reversed in comparison with that in cells where only CEACAM5 was silenced.

Cell cycle assays subsequently showed that the proportion of sh-CEACAM5-NC + sh-MDM2 cells in the S phase was reduced in comparison with that of sh-CEACAM5-NC + sh-MDM2-NC cells. Additionally, the proportion of sh-CEACAM5 + sh-MDM2-NC cells in the S phase was higher than that for sh-CEACAM5-NC + sh-MDM2 cells and was lower in sh-CEACAM5 + sh-MDM2 cells than in sh-CEACAM5 + sh-MDM2-NC cells. Finally, wound-healing assays showed that the migratory ability of sh-CEACAM5-NC + sh-MDM2 cells was reduced compared with that of sh-CEACAM5-NC + sh-MDM2-NC cells. Meanwhile, the migratory potential of sh-CEACAM5 + sh-MDM2-NC cells was greater than that of sh-CEACAM5-NC + sh-MDM2 cells and was lower in sh-CEACAM5 + sh-MDM2 cells than in sh-CEACAM5 + sh-MDM2-NC cells. In conclusion, the depletion of both MDM2 and CEACAM5 counteracted the inhibitory effect of CEACAM5 silencing on the EMT, resulting in EMT inhibition in HNSCC cells.

Discussion

Cancer-related morbidity and mortality are increasing rapidly worldwide [37,38]. While excessive smoking is associated with an increased incidence of HNSCC in developing countries, HPV infection is increasingly recognized as an important factor contributing to the increased incidence of oropharyngeal tumors in nonsmokers in developed countries [39]. The therapeutic modality of HPV-positive and HPV-negative HNSCC is essentially similar, including traditional surgical and chemoradiotherapy modalities, as well as new surgical techniques such as transoral robotic surgery and laser microsurgery [40]. The specific treatment plan depends on the site and stage of tumor development. OS for patients with HNSCC remains poor despite the advances in its diagnosis and treatment [41], while LN metastasis and extranodal extension are both important predictors of worse prognosis in HNSCC [42–44]. These observations underline the urgent need for further exploration of the mechanisms underlying HNSCC occurrence and

Clinical Science (2022) **136** 1691–1710
https://doi.org/10.1042/CS20220581

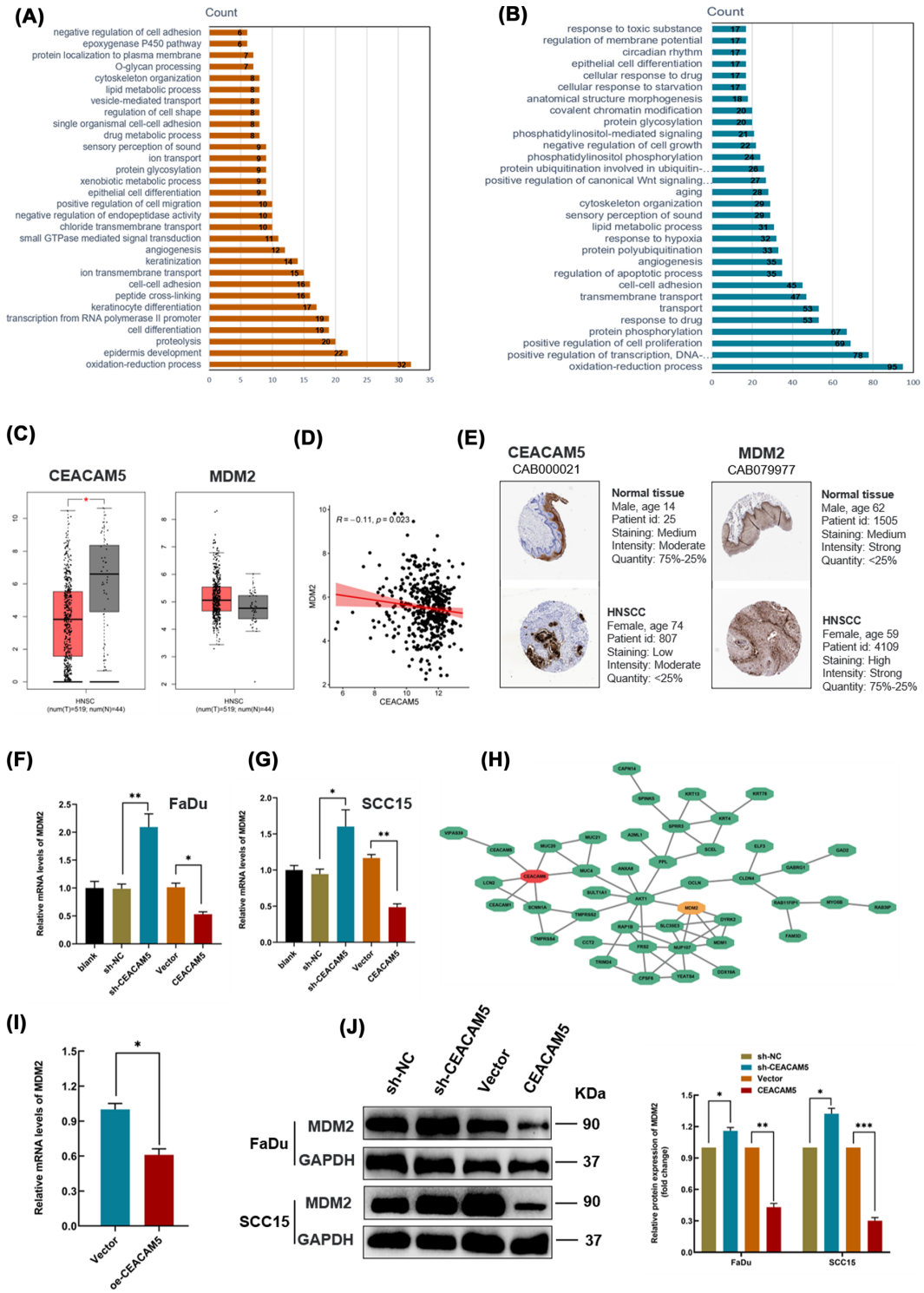

Figure 7. CEACAM5 inhibits the expression of MDM2

(**A,B**) Gene ontology (GO) terms related to the biological process (BP) category were assigned to genes associated with CEACAM5 and MDM2 based on HNSCC transcriptome-sequencing data. (**C,E**) The expression of CEACAM5 and MDM2 in normal and HNSCC tissues was analyzed based on data from TCGA. (**D**) Correlation analysis between MDM2 and CEACAM5 in HNSCC tissues based on data from TCGA (n=455). (**F,G**) The expression of MDM2 in HNSCC cells after stable lentivirus-mediated transduction was assessed by qRT-PCR. (**H**) PPI analysis was performed on genes related to the roles of CEACAM5 and MDM2 in HNSCC. (**I**) The mRNA expression levels of MDM2 in xenograft-derived tumors in nude mice were measured by qRT-PCR. (**J**) The protein expression of MDM2 in HNSCC cells was assessed by WB. The relevant statistics are shown in the right panel. *P<0.05, **P<0.01, ***P<0.001.

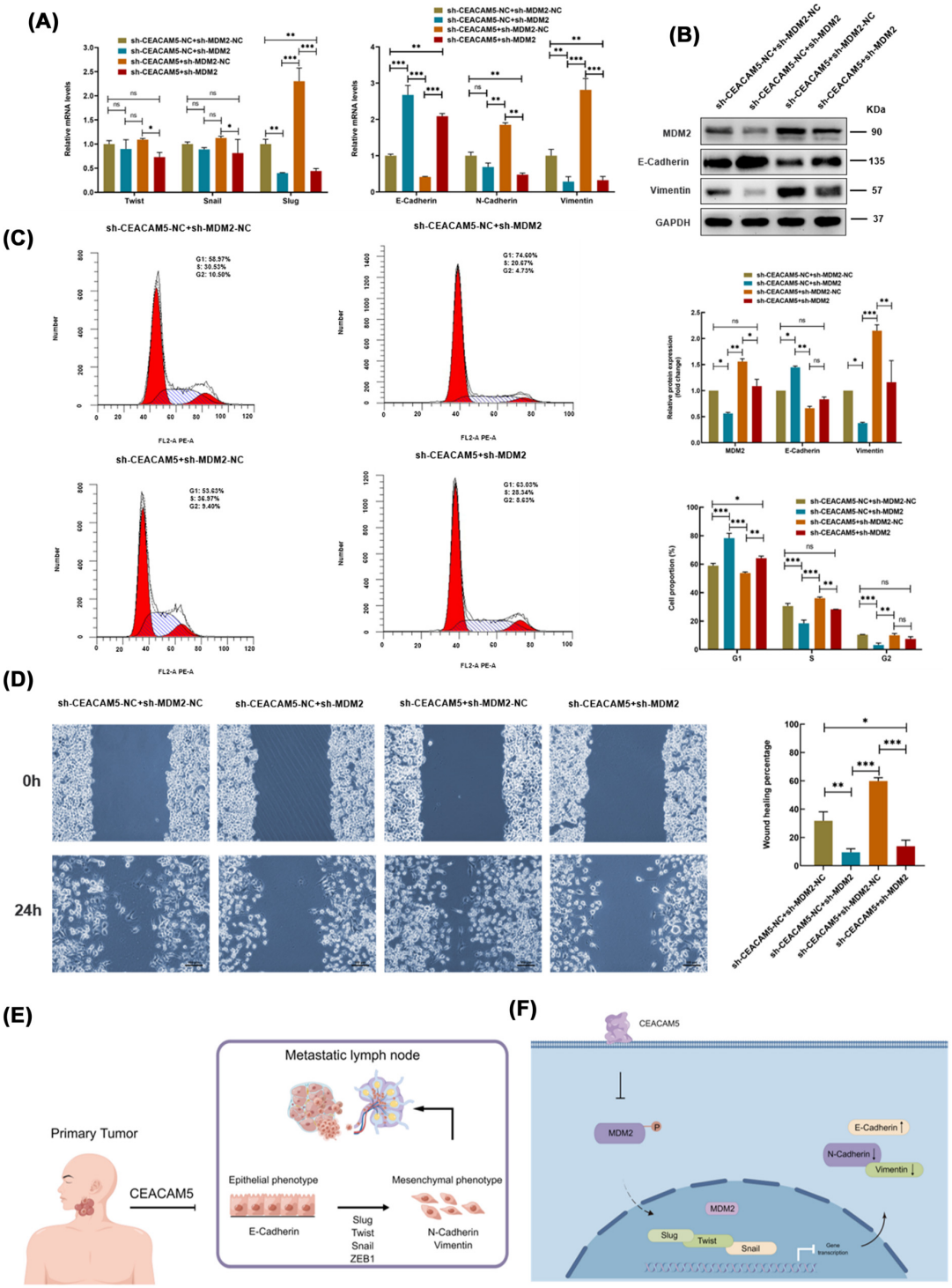

Figure 8. MDM2 knockdown reversed the effect of CEACAM5 silencing on the EMT

sh-MDM2-NC or sh-MDM2 was transfected into HNSCC cells after stable lentivirus-mediated transduction. (**A**) The mRNA levels of EMT-related transcription factors and biomarkers were measured by qRT-PCR. (**B**) The protein expression levels of MDM2 and EMT biomarkers were determined by WB. The relevant statistics are shown in the bottom panel. (**C**) Flow cytometry was used to detect the cell-cycle distribution of different cell lines. (**D**) The wound healing capacity of HNSCC cells transfected with sh-MDM2-NC or sh-MDM2 is shown. (**E,F**) Diagram showing the mechanism of the hypothesis postulated in the present study (generated by Figdraw). *P<0.05, **P<0.01, ***P<0.001; Abbreviation: NS, not significant.

Clinical Science (2022) **136** 1691–1710
https://doi.org/10.1042/CS20220581

progression, as well as identify novel targets and prognostic markers and develop effective strategies for the diagnosis and treatment of this cancer.

CEA was originally isolated from the blood of patients with colorectal cancer by Gold and Freedman [45]. The expression of this protein has since been observed to be up-regulated in many other human tumors, including pancreatic, lung, liver, gallbladder, breast, and bladder cancers, among others [46–48]. Accordingly, studies have mostly focused on its role as an oncogene in promoting cancer progression. In the present study, transcriptome sequencing in HNSCC tissues from patients with and without LN metastasis and analysis of high-throughput data downloaded from TCGA and GEO databases indicated that CEACAM5 expression was significantly reduced in HNSCC tumors compared with that in normal tissues. Generally, HPV-positive cases are more sensitive to chemoradiotherapy and, thus, have a better prognosis and a higher survival rate compared with HPV-negative cases [49]. However, in the present study, CEACAM5 expression was found to be higher in HPV-positive HNSCC than in HPV-negative HNSCC, and its expression level was also significantly lower in HNSCC tissues than in normal tissues, with a disease risk ratio of less than 1. This suggests that alterations in CEACAM5 expression are more likely to be a protective manifestation against this disease. Subsequently, survival analysis confirmed that elevated CEACAM5 expression was linked with improved OS, progression-free survival, DSS, and lower N-stage classification in patients with HNSCC.

p53 has been described as the guardian of the genome and controls multiple cellular processes, including DNA repair, cell-cycle arrest, apoptosis, autophagy, senescence, and metabolism through numerous mechanisms [50,51]. Ubiquitination is a reversible post-translational modification that modulates protein degradation and signal transduction through the binding of ubiquitin to protein substrates. This process mainly involves the E1-E2-E3 enzyme cascade and requires the activity of E1 ubiquitin-activating enzymes, E2 ubiquitin-conjugating enzymes, and E3 ubiquitin ligases. In addition, the regulation of NF-κB signaling by ubiquitination may be a potential therapeutic target for HNSCC [52]. MDM2 is an E3 ubiquitin ligase that can modulate p53 levels by promoting its degradation by the proteasome [53,54] or by binding to and stabilizing Slug mRNA independently of its ubiquitination activity, thereby stimulating cell invasion and metastasis [55–57]. Here, by analyzing transcriptome sequencing data to obtain DEGs and employing the STRING database to construct a PPI network, we found that CEACAM5 and MDM2 may have a negative regulatory relationship. Through the Network Analyst database, we assigned GO terms to genes associated with CEACAM5 and MDM2 expression and found similar enrichment patterns. In addition, analysis of TCGA dataset indicated that CEACAM5 and MDM2 expression exhibited opposing trends in HNSCC. Combined, these data suggested that CEACAM5 may regulate EMT processes by suppressing the expression of MDM2.

Malignant tumors induce lymphatic dilation (lymphangiogenesis) in the primary tumor and the drainage sentinel area by releasing lymphatic growth factors such as VEGF-C and LYVE1, thereby promoting LN metastasis [58–61]. Moreover, EMT is known to drive the metastasis of cervical cancer cells to LNs [62]. Here, we investigated the effect of CEACAM5 on LN metastasis *in vivo* using bioluminescence imaging and used IHC to assess the expression of LYVE1 in foot pad tumors derived from xenografted SCC15 cells in mice. The obtained results indicated that CEACAM5 overexpression abrogated the lymphatic metastasis of SCC15 cells. Despite our important findings, our study had several limitations. First, the number of samples used for transcriptomic analysis was small. Second, although our study indicated that CEACAM5 inhibits MDM2 expression in HNSCC, further investigation is required to clarify the specific underlying mechanisms.

In conclusion, this is the first study to show that CEACAM5 expression is down-regulated in HNSCC and that CEACAM5 expression is correlated with survival outcomes in HNSCC patients. CEACAM5 was also found to inhibit EMT in HNSCC cells by suppressing the expression of MDM2 and, ultimately, also LN metastasis. These findings contribute to the understanding of the molecular mechanism involved in HNSCC development.

Clinical perspectives

- Background: OS in patients with HNSCC remains poor despite the advances in its diagnosis and treatment. Additionally, both LN metastasis and extranodal extension are important predictors of the prognosis of this cancer.
- Results: Using *in vivo* and *in vitro* experiments as well as bioinformatics analysis, we found that CEACAM5 suppresses LN metastasis by suppressing EMT via inhibiting the expression of its downstream target MDM2.

- Significance: This is the first study to suggest that CEACAM5 may play a role in inhibiting LN metastasis and also provides a potential therapeutic target and prognostic marker for HNSCC.

Data Availability

All data generated or analyzed during the present study are included in this published article.

Competing Interests

The authors declare that there are no competing interests associated with the manuscript.

Funding

The present study was supported by the (National Natural Science Foundation of China) [grant number 82173303] and the (China Postdoctoral Science Foundation) [grant number 2021XM3029].

CRediT Author Contribution

Xudong Wang: Resources, Data curation, Software, Investigation, Visualization, Methodology, Writing—original draft. **Yanshi Li:** Software, Supervision. **Min Pan:** Validation, Writing—review & editing. **Tao Lu:** Software, Methodology. **Min Wang:** Formal Analysis. **Zhihai Wang:** Software. **Chuan Liu:** Methodology. **Guohua Hu:** Resources, Supervision, Project administration, Writing—review & editing.

Consent for Publication

Not applicable.

Ethics Statement

Clinical specimens were obtained from patients undergoing hypophargiectomy at the First Affiliated Hospital of Chongqing Medical University. Informed consent was obtained from each patient. Meanwhile, all mice were suffocated with 1% sodium pentobarbital plus a high concentration of carbon dioxide. All experiments in the present study were conducted in accordance with the Code of Ethics of the World Medical Association (Declaration of Helsinki). All protocols for clinical specimens and *in vivo* experiments in mice were approved by the Ethics Committee of the First Affiliated Hospital of Chongqing Medical University (2022-K184), and were conducted in accordance with the UK Animals (Scientific Procedures) Act and the National Institutes of Health guidelines.

Acknowledgements

Thanks to Molecular Medicine and Cancer Research Center of Chongqing Medical University for providing experimental equipment and experimental platform.

Abbreviations

BP, biological process; ANOVA, analysis of variance; PBS, phosphate buffered saline; SDS-PAGE, sodium dodecyl sulfate polyacrylamide gel electrophoresis; CEACAM5, carcinoembryonic antigen-related cell adhesion molecule 5; DEG, differentially expressed gene; EMT, epithelial–mesenchymal transition; FBS, fetal bovine serum; GEO, Gene Expression Omnibus; GPI, glycosylphosphatidylinositol; HNSCC, head and neck squamous cell carcinoma; HPV, human papillomavirus; IHC, immunohistochemistry; L, lymphatic metastasis; LM (+), lymphatic metastasis; LM (−), non-lymphatic metastasis; LN, lymph node; LYVE-1, lymphatic vessel endothelial hyaluronan receptor 1; MDM2, murine double minute 2; MOI, multiplicity of infection; NAT, normal adjacent tissue; NC, negative control; NL, no lymphatic metastasis; PPI, protein–protein interaction; qRT-PCR, quantitative reverse transcription-PCR; shRNA, short hairpin RNA; siRNA, small interfering RNA; T, tumor tissue; TCGA, The Cancer Genome Atlas; WB, western blotting.

References

1 Kang, H., Kiess, A. and Chung, C.H. (2015) Emerging biomarkers in head and neck cancer in the era of genomics. *Nat. Rev. Clin. Oncol.* **12**, 11–26, https://doi.org/10.1038/nrclinonc.2014.192

2 Panvongsa, W., Pegtel, D.M. and Voortman, J. (2022) More than a bubble: extracellular vesicle microRNAs in head and neck squamous cell carcinoma. *Cancers* **14**, 1160, https://doi.org/10.3390/cancers14051160

Clinical Science (2022) **136** 1691–1710
https://doi.org/10.1042/CS20220581

3 Ferlay, J., Colombet, M., Soerjomataram, I., Mathers, C., Parkin, D.M., Pineros, M. et al. (2019) Estimating the global cancer incidence and mortality in 2018: GLOBOCAN sources and methods. *Int. J. Cancer* **144**, 1941–1953, https://doi.org/10.1002/ijc.31937
4 Johnson, D.E., Burtness, B., Leemans, C.R., Lui, V.W.Y., Bauman, J.E. and Grandis, J.R. (2020) Head and neck squamous cell carcinoma. *Nat. Rev. Dis. Primers* **6**, 92, https://doi.org/10.1038/s41572-020-00224-3
5 Seiwert, T.Y., Zuo, Z.X., Keck, M.K., Khattri, A., Pedamallu, C.S., Stricker, T. et al. (2015) Integrative and comparative genomic analysis of HPV-positive and HPV-negative head and neck squamous cell carcinomas. *Clin. Cancer Res.* **21**, 632–641, https://doi.org/10.1158/1078-0432.CCR-13-3310
6 Zhang, X.-m., Han, W.-x., Wang, H.-y. and He, Q. (2017) Correlation between lymphatic endothelial markers and lymph node status or N-staging of colorectal cancer. *World J. Surg. Oncol.* **15**, 204, https://doi.org/10.1186/s12957-017-1276-3
7 Xing, Y., Zhang, J., Lin, H., Gold, K.A., Sturgis, E.M., Garden, A.S. et al. (2016) Relation between the level of lymph node metastasis and survival in locally advanced head and neck squamous cell carcinoma. *Cancer* **122**, 534–545, https://doi.org/10.1002/cncr.29780
8 Shah, J.P., Shaha, A.R., Spiro, R.H. and Strong, E.W. (1976) Carcinoma of the hypopharynx. *Am. J. Surg.* **132**, 439–443, https://doi.org/10.1016/0002-9610(76)90315-9
9 Amit, M., Liu, C., Gleber-Netto, F.O., Kini, S., Tam, S., Benov, A. et al. (2021) Inclusion of extranodal extension in the lymph node classification of cutaneous squamous cell carcinoma of the head and neck. *Cancer* **127**, 1238–1245, https://doi.org/10.1002/cncr.33373
10 Licitra, L., Locati, L.D. and Bossi, P. (2004) Head and neck cancer. *Ann. Oncol.* **15**, 267–273, https://doi.org/10.1093/annonc/mdh937
11 Karam, S.D. and Raben, D. (2019) Radioimmunotherapy for the treatment of head and neck cancer. *Lancet Oncol.* **20**, E404–E416, https://doi.org/10.1016/S1470-2045(19)30306-7
12 Budach, V. and Tinhofer, I. (2019) Novel prognostic clinical factors and biomarkers for outcome prediction in head and neck cancer: a systematic review. *Lancet Oncol.* **20**, E313–E326, https://doi.org/10.1016/S1470-2045(19)30177-9
13 Mroz, E.A., Tward, A.M., Hammon, R.J., Ren, Y. and Rocco, J.W. (2015) Intra-tumor genetic heterogeneity and mortality in head and neck cancer: analysis of data from The Cancer Genome Atlas. *PLoS Med.* **12**, e1001786, https://doi.org/10.1371/journal.pmed.1001786
14 Byron, S.A., Van Keuren-Jensen, K.R., Engelthaler, D.M., Carpten, J.D. and Craig, D.W. (2016) Translating RNA sequencing into clinical diagnostics: opportunities and challenges. *Nat. Rev. Genet.* **17**, 257–271, https://doi.org/10.1038/nrg.2016.10
15 Peng, J., Sun, B.-F., Chen, C.-Y., Zhou, J.-Y., Chen, Y.-S., Chen, H. et al. (2019) Single-cell RNA-seq highlights intra-tumoral heterogeneity and malignant progression in pancreatic ductal adenocarcinoma. *Cell Res.* **29**, 725–738, https://doi.org/10.1038/s41422-019-0195-y
16 Papalexi, E. and Satija, R. (2018) Single-cell RNA sequencing to explore immune cell heterogeneity. *Nat. Rev. Immunol.* **18**, 35–45, https://doi.org/10.1038/nri.2017.76
17 Hong, M., Tao, S., Zhang, L., Diao, L.-T., Huang, X., Huang, S. et al. (2020) RNA sequencing: new technologies and applications in cancer research. *J. Hematol. Oncol.* **13**, 166, https://doi.org/10.1186/s13045-020-01005-x
18 Zheng, Y. and Yang, X. (2022) Application and prospect of single-cell sequencing in cancer metastasis. *Fut. Oncol.* **18**, 2723–2736, https://doi.org/10.2217/fon-2022-0156
19 Puram, S.V., Tirosh, I., Parikh, A.S., Patel, A.P., Yizhak, K., Gillespie, S. et al. (2017) Single-cell transcriptomic analysis of primary and metastatic tumor ecosystems in head and neck cancer. *Cell* **171**, 1611–+, https://doi.org/10.1016/j.cell.2017.10.044
20 Blumenthal, R.D., Hansen, H.J. and Goldenberg, D.M. (2005) Inhibition of adhesion, invasion, and metastasis by antibodies targeting CEACAM6 (NCA-90) and CEACAM5 (Carcinoembryonic antigen). *Cancer Res.* **65**, 8809–8817, https://doi.org/10.1158/0008-5472.CAN-05-0420
21 Saeland, E., Belo, A.I., Mongera, S., van Die, I., Meijer, G.A. and van Kooyk, Y. (2012) Differential glycosylation of MUC1 and CEACAM5 between normal mucosa and tumour tissue of colon cancer patients. *Int. J. Cancer* **131**, 117–128, https://doi.org/10.1002/ijc.26354
22 Blumenthal, R.D., Leon, E., Hansen, H.J. and Goldenberg, D.M. (2007) Expression patterns of CEACAM5 and CEACAM6 in primary and metastatic cancers. *BMC Cancer* **7**, 2, https://doi.org/10.1186/1471-2407-7-2
23 Wade, M., Li, Y.-C. and Wahl, G.M. (2013) MDM2 MDMX and p53 in oncogenesis and cancer therapy. *Nat. Rev. Cancer* **13**, 83–96, https://doi.org/10.1038/nrc3430
24 Jung, C.-H., Kim, J., Park, J.K., Hwang, S.-G., Moon, S.-K., Kim, W.-J. et al. (2013) Mdm2 increases cellular invasiveness by binding to and stabilizing the Slug mRNA. *Cancer Lett.* **335**, 270–277, https://doi.org/10.1016/j.canlet.2013.02.035
25 Lamouille, S., Xu, J. and Derynck, R. (2014) Molecular mechanisms of epithelial-mesenchymal transition. *Nat. Rev. Mol. Cell Biol.* **15**, 178–196, https://doi.org/10.1038/nrm3758
26 Wang, X., Xu, X., Peng, C., Qin, Y., Gao, T., Jing, J. et al. (2019) BRAF(V600E)-induced KRT19 expression in thyroid cancer promotes lymph node metastasis via EMT. *Oncol. Lett.* **18**, 927–935, https://doi.org/10.3892/ol.2019.10360
27 Pastushenko, I. and Blanpain, C. (2019) EMT transition states during tumor progression and metastasis. *Trends Cell Biol.* **29**, 212–226, https://doi.org/10.1016/j.tcb.2018.12.001
28 Karlsson, M.C., Gonzalez, S.F., Welin, J. and Fuxe, J. (2017) Epithelial-mesenchymal transition in cancer metastasis through the lymphatic system. *Mol. Oncol.* **11**, 781–791, https://doi.org/10.1002/1878-0261.12092
29 Liu, K., Xue, B., Bai, G. and Zhang, W. (2020) F-box protein FBXO31 modulates apoptosis and epithelial-mesenchymal transition of cervical cancer via inactivation of the PI3K/AKT-mediated MDM2/p53 axis. *Life Sci.* **259**, 118277, https://doi.org/10.1016/j.lfs.2020.118277
30 De Craene, B. and Berx, G. (2013) Regulatory networks defining EMT during cancer initiation and progression. *Nat. Rev. Cancer* **13**, 97–110, https://doi.org/10.1038/nrc3447
31 Li, Y., Lu, T. and Hu, G. (2020) Gene sequencing and expression of Raf-1 in lymphatic metastasis of hypopharyngeal carcinoma. *Cancer Biomark.* **28**, 181–191, https://doi.org/10.3233/CBM-191238
32 Szklarczyk, D., Gable, A.L., Nastou, K.C., Lyon, D., Kirsch, R., Pyysalo, S. et al. (2021) The STRING database in 2021: customizable protein-protein networks, and functional characterization of user-uploaded gene/measurement sets. *Nucleic. Acids. Res.* **49**, D605–D612, https://doi.org/10.1093/nar/gkaa1074

33 Shannon, P., Markiel, A., Ozier, O., Baliga, N.S., Wang, J.T., Ramage, D. et al. (2003) Cytoscape: a software environment for integrated models of biomolecular interaction networks. *Genome Res.* **13**, 2498–2504, https://doi.org/10.1101/gr.1239303
34 Zhou, G., Soufan, O., Ewald, J., Hancock, R.E.W., Basu, N. and Xia, J. (2019) NetworkAnalyst 3.0: a visual analytics platform for comprehensive gene expression profiling and meta-analysis. *Nucleic. Acids. Res.* **47**, W234–W241, https://doi.org/10.1093/nar/gkz240
35 Chibaya, L., Karim, B., Zhang, H. and Jones, S.N. (2021) Mdm2 phosphorylation by Akt regulates the p53 response to oxidative stress to promote cell proliferation and tumorigenesis. *Proc. Natl. Acad. Sci. U.S.A.* **118**, e2003193118, https://doi.org/10.1073/pnas.2003193118
36 Carr, M.I., Roderick, J.E., Gannon, H.S., Kelliher, M.A. and Jones, S.N. (2016) Mdm2 phosphorylation regulates its stability and has contrasting effects on oncogene and radiation-induced tumorigenesis. *Cell Reports* **16**, 2618–2629, https://doi.org/10.1016/j.celrep.2016.08.014
37 Sung, H., Ferlay, J., Siegel, R.L., Laversanne, M., Soerjomataram, I., Jemal, A. et al. (2021) Global cancer statistics 2020: GLOBOCAN estimates of incidence and mortality worldwide for 36 cancers in 185 countries. *CA Cancer J. Clin.* **71**, 209–249, https://doi.org/10.3322/caac.21660
38 Hirshoren, N., Danne, J., Dixon, B.J., Magarey, M., Kleid, S., Webb, A. et al. (2017) Prognostic markers in metastatic cutaneous squamous cell carcinoma of the head and neck. *Head Neck-J. Sci. Spec. Head Nec.* **39**, 772–778, https://doi.org/10.1002/hed.24683
39 Lawrence, M.S., Sougnez, C., Lichtenstein, L., Cibulskisl, K., Lander, E., Gabriel, S.B. et al. (2015) Comprehensive genomic characterization of head and neck squamous cell carcinomas. *Nature (London)* **517**, 576–582, https://doi.org/10.1038/nature14129
40 Nichols, D.S., Zhao, J., Boyce, B.J., Amdur, R., Mendenhall, W.M., Danan, D. et al. (2021) HPV/p16-positive oropharyngeal cancer treated with transoral robotic surgery: The roles of margins, extra-nodal extension and adjuvant treatment. *Am. J. Otolaryngol.* **42**, 102793, https://doi.org/10.1016/j.amjoto.2020.102793
41 Hsieh, R.W., Borson, S., Tsagianni, A. and Zandberg, D.P. (2021) Immunotherapy in recurrent/metastatic squamous cell carcinoma of the head and neck. *Front. Oncol.* **11**, 705614, https://doi.org/10.3389/fonc.2021.705614
42 Matsumoto, F., Mori, T., Matsumura, S., Matsumoto, Y., Fukasawa, M., Teshima, M. et al. (2017) Prognostic significance of surgical extranodal extension in head and neck squamous cell carcinoma patients. *Jpn. J. Clin. Oncol.* **47**, 699–704, https://doi.org/10.1093/jjco/hyx055
43 Lydiatt, W.M., Patel, S.G., O'Sullivan, B., Brandwein, M.S., Ridge, J.A., Migliacci, J.C. et al. (2017) Head and neck cancers-major changes in the American Joint Committee on Cancer Eighth Edition Cancer Staging Manual. *CA Cancer J. Clin.* **67**, 122–137, https://doi.org/10.3322/caac.21389
44 Melkane, A.E., Mamelle, G., Wycisk, G., Temam, S., Janot, F., Casiraghi, O. et al. (2012) Sentinel node biopsy in early oral squamous cell carcinomas: a 10-year experience. *Laryngoscope* **122**, 1782–1788, https://doi.org/10.1002/lary.23383
45 Chan, C.H.F. and Stanners, C.P. (2007) Recent advances in the tumour biology of the GPI-anchored carcinoembryonic antigen family members CEACAM5 and CEACAM6. *Curr. Oncol. (Toronto, Ont.)* **14**, 70–73, https://doi.org/10.3747/co.2007.109
46 Wang, X.-M., Zhang, Z., Pan, L.-H., Cao, X.-C. and Xiao, C. (2019) KRT19 and CEACAM5 mRNA-marked circulated tumor cells indicate unfavorable prognosis of breast cancer patients. *Breast Cancer Res. Treat.* **174**, 375–385, https://doi.org/10.1007/s10549-018-05069-9
47 DeLucia, D.C., Cardillo, T.M., Ang, L., Labrecque, M.P., Zhang, A., Hopkins, J.E. et al. (2021) Regulation of CEACAM5 and therapeutic efficacy of an anti-CEACAM5-SN38 antibody-drug conjugate in neuroendocrine prostate cancer. *Clin. Cancer Res.* **27**, 759–774, https://doi.org/10.1158/1078-0432.CCR-20-3396
48 Baek, D.-S., Kim, Y.-J., Vergara, S., Conard, A., Adams, C., Calero, G. et al. (2022) A highly-specific fully-human antibody and CAR-T cells targeting CD66e/ CEACAM5 are cytotoxic for CD66e-expressing cancer cells in vitro and in vivo. *Cancer Lett.* **525**, 97–107, https://doi.org/10.1016/j.canlet.2021.10.041
49 Ochoa, I.S., O'Regan, E., Toner, M., Kay, E., Faul, P., O'Keane, C. et al. (2022) The role of HPV in determining treatment, survival, and prognosis of head and neck squamous cell carcinoma. *Cancers* **14**, 4321, https://doi.org/10.3390/cancers14174321
50 Koo, N., Sharma, A.K. and Narayan, S. (2022) Therapeutics targeting p53-MDM2 interaction to induce cancer cell death. *Int. J. Mol. Sci.* **23**, 5005, https://doi.org/10.3390/ijms23095005
51 Cheng, F., Dou, J., Zhang, Y., Wang, X., Wei, H., Zhang, Z. et al. (2021) Urolithin A inhibits epithelial-mesenchymal transition in lung cancer cells via P53-MDM2-snail pathway. *Onco. Targets Ther.* **14**, 3199–3208, https://doi.org/10.2147/OTT.S305595
52 Morgan, E.L., Chen, Z. and Van Waes, C. (2020) Regulation of NF kappa B signalling by ubiquitination: a potential therapeutic target in head and neck squamous cell carcinoma? *Cancers* **12**, 2877, https://doi.org/10.3390/cancers12102877
53 Sun, C., Li, M., Zhang, L., Sun, F., Chen, H., Xu, Y. et al. (2022) IDO1 plays a tumor-promoting role via MDM2-mediated suppression of the p53 pathway in diffuse large B-cell lymphoma. *Cell Death Dis.* **13**, 572, https://doi.org/10.1038/s41419-022-05021-2
54 Chene, P. (2003) Inhibiting the p53-MDM2 interaction: An important target for cancer therapy. *Nat. Rev. Cancer* **3**, 102–109, https://doi.org/10.1038/nrc991
55 Zhou, G., Zhai, Y., Cui, Y., Zhang, X., Dong, X., Yang, H. et al. (2007) MDM2 promoter SNP309 is associated with risk of occurrence and advanced lymph node metastasis of nasopharyngeal carcinoma in Chinese population. *Clin. Cancer Res.* **13**, 2627–2633, https://doi.org/10.1158/1078-0432.CCR-06-2281
56 Zhang, F., Xu, Y., Ye, W., Jiang, J. and Wu, C. (2020) Circular RNA S-7 promotes ovarian cancer EMT via sponging miR-641 to up-regulate ZEB1 and MDM2. *Biosci. Rep.* **40**, BSR20200825, https://doi.org/10.1042/BSR20200825
57 Wang, S.-P., Wang, W.-L., Chang, Y.-L., Wu, C.-T., Chao, Y.-C., Kao, S.-H. et al. (2009) p53 controls cancer cell invasion by inducing the MDM2-mediated degradation of Slug. *Nat. Cell Biol.* **11**, 694–704, https://doi.org/10.1038/ncb1875
58 Tyagi, A. (2022) Underlying facets of cancer metastasis. *Cancers* **14**, 2989, https://doi.org/10.3390/cancers14122989
59 Stacker, S.A., Williams, S.P., Karnezis, T., Shayan, R., Fox, S.B. and Achen, M.G. (2014) Lymphangiogenesis and lymphatic vessel remodelling in cancer. *Nat. Rev. Cancer* **14**, 159–172, https://doi.org/10.1038/nrc3677
60 Sainz-Jaspeado, M. and Claesson-Welsh, L. (2018) Cytokines regulating lymphangiogenesis. *Curr. Opin. Immunol.* **53**, 58–63, https://doi.org/10.1016/j.coi.2018.04.003
61 Karaman, S. and Detmar, M. (2014) Mechanisms of lymphatic metastasis. *J. Clin. Invest.* **124**, 922–928, https://doi.org/10.1172/JCI71606

Clinical Science (2022) **136** 1691–1710
https://doi.org/10.1042/CS20220581

62 Liao, Y., Huang, J., Liu, P., Zhang, C., Liu, J., Xia, M. et al. (2022) Downregulation of LNMAS orchestrates partial EMT and immune escape from macrophage phagocytosis to promote lymph node metastasis of cervical cancer. *Oncogene* **41**, 1931–1943, https://doi.org/10.1038/s41388-022-02202-3